

Neutron Spectroscopic Evidence for Cluster Formation and Percolative Superconductivity in $\text{ErBa}_2\text{Cu}_3\text{O}_x$

J. Mesot, P. Allenspach, U. Staub, and A. Furrer

Laboratory for Neutron Scattering, Eidgenössische Technische Hochschule Zürich, CH-5232 Villigen PSI, Switzerland

H. Mutka

Institut Laue-Langevin, 156 X, F-38042 Grenoble CEDEX, France

(Received 9 June 1992)

Inelastic neutron scattering has been employed to study in detail the low-energy crystal-field excitations of Er^{3+} in $\text{ErBa}_2\text{Cu}_3\text{O}_x$ ($6 < x < 7$). The observed energy spectra are found to be the result of a superposition of three stable states, which we interpret in terms of local regions of semiconducting and metallic character. The superconductivity is shown to result from the formation of a two-dimensional percolative network. A two-dimensional bond percolation model correctly predicts the critical oxygen contents associated with the two-plateau structure of T_c .

PACS numbers: 74.72.Jt, 71.70.Ch

One of the most interesting aspects of the superconductivity in the perovskite-type compounds $R\text{Ba}_2\text{Cu}_3\text{O}_x$ (R = rare earth or yttrium, $6 < x < 7$) is the relation between T_c and the oxygen stoichiometry. Annealed systems show the well-known two-plateau structure of T_c . While $T_c \approx 90$ K for $7.0 \geq x \geq 6.8$, it drops to about 60 K for $6.7 \geq x \geq 6.4$, and the superconductivity is totally suppressed for $x < 6.4$. It is now generally believed that the superconducting properties are related to both the oxygen concentration and the oxygen ordering in the basal plane. Another important feature is the effect of phase separation which generates a coexistence of two different structural phases. Phase separation has been observed for $\text{La}_{2-x}\text{Sr}_x\text{CuO}_{4+\delta}$, the parent compound for the layered copper oxide systems, by neutron diffraction experiments on polycrystalline [1] and single-crystalline [2] materials, ^{139}La NMR studies [3], and field-dependent magnetization measurements [4]. Radaelli *et al.* have recently observed similar effects for $\text{ErBa}_2\text{Cu}_3\text{O}_x$ in the vicinity of the tetragonal to orthorhombic phase transformation [5]. There are a number of theoretical papers dealing with the phase separation problem in high- T_c superconductors, too [6–8]. Based on the observation of the crystalline-electric-field (CEF) interaction at the Er^{3+} site in $\text{ErBa}_2\text{Cu}_3\text{O}_x$ as a function of the oxygen content x , we provide in this Letter direct experimental evidence for the formation of three different types of clusters in the superconducting CuO_2 planes. In particular, the observed energy spectra are interpreted as a superposition of two different metallic components and a semiconducting one, the relative weight of each component being extremely dependent upon the oxygen concentration x . The superconductivity can be shown to result from the formation of a two-dimensional percolative network, with the two-plateau structure of T_c being directly related to the variation of the proportions of the different cluster types versus the oxygen content x .

In most high- T_c compounds the rare-earth ions are sit-

uated close to the CuO_2 planes where it is widely believed that the superconducting carriers are located; thus the CEF interaction at the R site constitutes an ideal probe of the local symmetry and the charge distribution of the superconducting CuO_2 planes and thereby monitors directly changes of the carrier concentration induced, e.g., by oxygen nonstoichiometry, pressure, doping, and disordering effects. Very detailed and direct information about the CEF interaction results from inelastic neutron scattering (INS) experiments, particularly for optically opaque materials like the high- T_c compounds. Recently we have established in detail the CEF level structure of $\text{ErBa}_2\text{Cu}_3\text{O}_x$, and we have been able to derive quantitative information on the charge transfer upon oxygen reduction and doping (at the Cu sites) from the experimentally determined CEF parameters [9–11]. In particular, we have been able to observe all the seven excited CEF states of Er^{3+} in $\text{ErBa}_2\text{Cu}_3\text{O}_x$ resulting from the decomposition of the sixteenfold degenerate ground-state J -multiplet $^4I_{15/2}$ due to the CEF interaction of either orthorhombic or tetragonal symmetry. All the CEF transitions were characterized by a monotonic behavior of their energies versus the oxygen content x , with the exception of the lowest-lying CEF state which was found to behave in a totally anomalous way. Therefore we investigated the low-energy CEF excitations of $\text{ErBa}_2\text{Cu}_3\text{O}_x$ in more detail under improved resolution conditions as discussed below.

The polycrystalline $\text{ErBa}_2\text{Cu}_3\text{O}_x$ samples were the same as those used in our previous INS experiments [9,11]. The sample preparation has been described in detail elsewhere [12,13]. We treated the powdered material by a temperature controlled desorption-absorption procedure to yield the final oxygen contents of $x = 6.09, 6.34, 6.45, 6.53, 6.78, 6.91,$ and 6.98 . The samples were annealed from 920°C to room temperature at a rate of $1^\circ\text{C}/\text{mm}$, but the cooling process was interrupted several times for a period of 5 h at 800, 600, 400, and 200°C in

order to improve the thermal equilibrium with regard to the oxygen occupancies. Neutron diffraction proved the crystallographic single-phase character of the samples, and the two-plateau structure of T_c was established by dc magnetic susceptibility measurements. The INS experiments were performed with use of the time-of-flight spectrometer IN4 at the high-flux reactor of the Institut Laue-Langevin (ILL) at Grenoble with an incident neutron energy of 17.21 meV. Using a very good collimation we achieved an instrumental resolution (FWHM) of 0.3 meV for energy transfers $7 \leq \Delta E \leq 11$ meV. The samples were enclosed into cylindrical aluminum containers of 10 mm diam and 50 mm height which were mounted in a helium cryostat to achieve temperatures $T > 10$ K. The raw data have been corrected for absorption, detector efficiency, background, and phase space effects by standard procedures.

The observed energy spectra covering the ground-state transitions to the three lowest CEF states of $\text{ErBa}_2\text{Cu}_3\text{O}_x$ are shown in Fig. 1. The evolution of the scattering versus the oxygen content x behaves differently for the three CEF transitions A , B , and C . While the energies of the CEF transitions B and C are almost independent of x

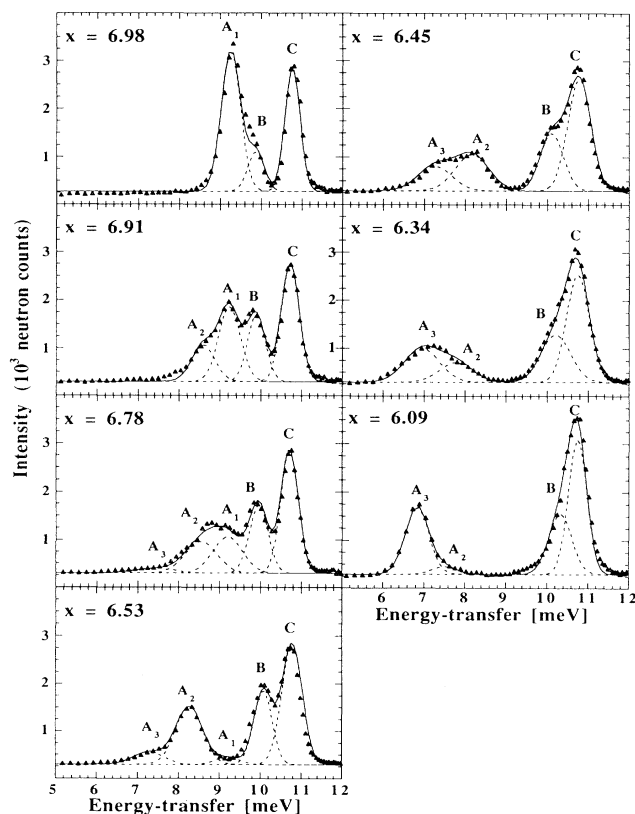


FIG. 1. Energy spectra of neutrons scattered from $\text{ErBa}_2\text{Cu}_3\text{O}_x$ at $T=10$ K. The lines are the result of a least-squares fitting procedure as explained in the text.

and their intensities are slowly increasing when going from $x=7$ to $x=6$, the x dependence of the CEF transition A exhibits a most unusual behavior: Not only do we observe a major shift to lower energies and a significant decrease of the line intensity upon lowering the oxygen content x , but also there is evidence for real substructures associated with the CEF transition A . More specifically, the CEF transition A appears to be decomposed into three individual transitions A_1 , A_2 , and A_3 , whose spectral weights distinctly depend on the oxygen content x .

We now proceed to analyze the energy spectra of Fig. 1 in detail. In our earlier work [9,11] we have determined the CEF parameters of $\text{ErBa}_2\text{Cu}_3\text{O}_x$ for each oxygen content on the basis of the average energies and intensities of the seven ground-state transitions. From these results we found that the matrix element of the CEF transition A decreases smoothly with decreasing energy. In the analysis of the energy spectra of Fig. 1 the relative strengths of the lines A ($A=A_1+A_2+A_3$), B , and C and their centers of gravity were kept fixed at the transition matrix elements and energies resulting from the previously determined CEF parameters [9,11], respectively. The only fitting parameters were then a scaling factor for the intensity, two linewidth parameters (one for the transitions A_i and one for the transitions B and C), and three positional parameters for the CEF transitions A_i . All the transitions are approximated by Gaussian functions; thus the linewidth can be expressed as a quadratic sum of both intrinsic and instrumental contributions. We arrive at a decomposition of the observed energy spectra as indicated by the dashed lines in Fig. 1 which are found to be in excellent agreement with the experimental data. The main results can be summarized as follows.

(1) Intensities: The transitions A_1 , A_2 , and A_3 have maximum weight close to $x=7.0$, $x=6.5$, and $x=6.0$, respectively. With the CEF interaction being a local probe, there is no doubt that the above substructures originate from different local environments of the Er^{3+} ions which obviously coexist in the compound $\text{ErBa}_2\text{Cu}_3\text{O}_x$.

(2) Energies: Whereas all the CEF transitions are independent of energy for oxygen content $x \geq 6.5$ within the experiment error, they shift slightly when going from $x \approx 6.5$ to $x \approx 6.0$. This may be due to the structural discontinuities at the orthorhombic to tetragonal phase transition at $x \approx 6.4$.

(3) Linewidth: As visualized in Fig. 2 the intrinsic linewidths of the transitions A_i are much smaller for oxygen contents where these transitions individually reach their maximum weight, namely, for $x \approx 6.0$, 6.5 , and 7.0 . The linewidths obviously reflect the structural homogeneity around the Er^{3+} ions which is well defined when only one particular cluster type dominates. The linewidths of the transitions B and C vary in a similar (though less pronounced) manner. The rather high degree of homogeneity around $x \approx 6.5$ is certainly related to superlattice ordering of the CuO chains as observed

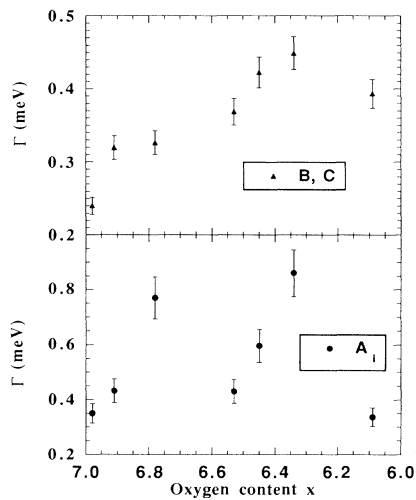


FIG. 2. Intrinsic linewidths of the CEF transitions A_i , B , and C determined for $\text{ErBa}_2\text{Cu}_3\text{O}_x$ at $T=10$ K.

around $x \approx 6.5$ by electron microscopy [14] or deduced by neutron diffraction [15].

Our data and their interpretation provide clear experimental evidence for cluster formation. It is tempting to identify the three clusters associated with the transitions A_1 , A_2 , and A_3 by two local regions of metallic ($T_c \approx 90$ K, $T_c \approx 60$ K) and a local region of semiconducting character, respectively. In order to derive correctly the x -dependent fractional proportions of the three cluster types, the intensities of the transitions A_i have to be corrected by the corresponding matrix elements of each component by interpolating this function of energy (as mentioned above, the matrix element for the CEF transition A varies smoothly with energy).

Figure 3 shows the fractional proportions of the three cluster types which exhibit a continuous behavior versus the oxygen content x , consistent with our earlier findings that the transfer of holes into the CuO_2 planes is linearly related to the oxygenation process [9,11]. This is in agreement with the bond valence sum arguments derived from neutron diffraction experiments on $\text{ErBa}_2\text{Cu}_3\text{O}_x$ which give evidence for a linear decrease of the c axis upon hole doping [5], but in contrast to the conclusions of similar experiments on $\text{YBa}_2\text{Cu}_3\text{O}_x$ where the semiconductor-metal transition has been suggested to be due to the nonlinearity of the hole transfer into the planes [16]. Furthermore, the continuous increase of the metallic states A_1 and A_2 can explain the increase of the superconducting volume fraction as observed by magnetic susceptibility measurements [5] when the oxygen content is raised from $x=6$ to $x=7$.

Our current understanding of the superconducting properties of $\text{ErBa}_2\text{Cu}_3\text{O}_x$ (and more generally all the $\text{RBa}_2\text{Cu}_3\text{O}_x$ compounds) involves a percolation mechanism of electric conductivity as recently discussed in both

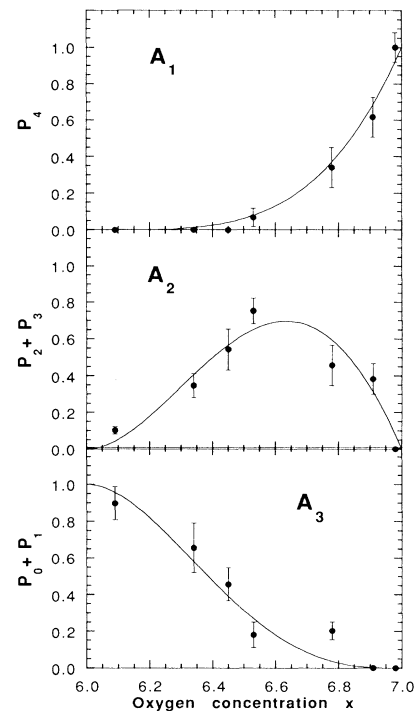


FIG. 3. Proportions of the lowest-lying CEF transitions A_i of $\text{ErBa}_2\text{Cu}_3\text{O}_x$ as a function of the oxygen content x . The lines refer to geometrical probability functions as explained in the text.

theoretical [6] and experimental [4] work. For $x=6$ the system is a perfect semiconductor. When adding oxygen ions into the chains, holes are continuously transferred into the CuO_2 planes [9,11]. By this mechanism the number of local regions with metallic character (associated with the CEF transition A_2) rises, which can partially combine to form larger regions. For some critical concentration a percolative network is built up, and the system undergoes a transition from the semiconducting to the conducting state (with $T_c \approx 60$ K). Upon further increasing the hole concentration a second (different) type of metallic cluster (associated with the CEF transition A_1) is formed; these start to attach to each other and at the percolation limit induce a transition into another conducting state (with $T_c \approx 90$ K). For a two-dimensional square structure the critical concentration for bond percolation is $p_c=50\%$ [17]. From the fractional proportions of A_2 and A_1 displayed in Fig. 3 we can then immediately determine the critical oxygen concentrations for the transitions from the semiconducting to the $T_c \approx 60$ K superconducting state and to the $T_c \approx 90$ K superconducting state to be $x_2=6.42$ and $x_1=6.86$, respectively, which is in excellent agreement with the observed two-plateau structure of T_c [13,16]. For three-dimensional structures, on the other hand, the critical concentration for bond percolation is 20% (face-centered

cubic) $< p_c < 30\%$ (simple cubic) [17]. From Fig. 3 we derive $6.21 < x_2 < 6.31$ and $6.64 < x_1 < 6.73$, which is inconsistent with the observed two-plateau structure of T_c . This reinforces the well-known fact that the superconductivity in the perovskite-type compounds has indeed a two-dimensional character. A similar percolation model based on oxygen ordering effects in the CuO chains and the presence of oxygen-poor regions acting as superconducting grain boundaries gives a critical value $x_1 = 6.74$ [8,18].

Combined statistical and geometrical considerations may be useful to understand the x -dependent profiles of the fractional proportions of the three cluster types visualized in Fig. 3. In an earlier publication [19] we have developed a local symmetry model and defined the following probabilities $P_k(y)$ to have, for a given oxygen content $x = 6 + y$, k of the four oxygen chain sites $(0, \frac{1}{2}, 0)$, $(1, \frac{1}{2}, 0)$, $(0, \frac{1}{2}, 1)$, and $(1, \frac{1}{2}, 1)$ nearest to the Er^{3+} ion occupied:

$$P_k(y) = \binom{4}{k} y^k (1-y)^{4-k}, \quad (0 \leq k \leq 4). \quad (1)$$

The fractional proportion of the cluster type A_1 exhibits the behavior predicted by the probability function $P_4(y)$ (i.e., all the oxygen chain sites being occupied). Similarly, the fractional proportions of the cluster types A_2 and A_3 follow the sum of the probability functions $P_3(y) + P_2(y)$ (i.e., one or two empty oxygen chain sites) and $P_1(y) + P_0(y)$ (i.e., one or none oxygen chain site being occupied), respectively. The above probability functions are shown in Fig. 3 by solid lines which excellently reproduce the experimental data. However, it is not yet clear whether this agreement is accidental or physically meaningful.

Finally we emphasize the role of neutron CEF spectroscopy among all experimental techniques as a unique and powerful tool to probe directly the local electronic configurations of the high- T_c perovskite-type compounds. Any attempts to unravel cluster formation effects in these compounds, for example, by diffraction measurements, are likely to fail due to the rather small localization range anticipated for the different clusters. Indeed, a recently proposed ferromagnetic cluster model [6] predicts the local phases in the $\text{La}_{2-x}(\text{Ba},\text{Sr})_x\text{CuO}_4$ and $R\text{Ba}_2\text{Cu}_3\text{O}_x$ compounds to include thirteen and five plane copper ions, respectively, i.e., the localization range is restricted to a few unit cells only. While the semiconducting to metal transition may also be understood and related to the recently reported phase separation effects at $x \approx 6.4$ [5], the coexistence of two different types of metallic clusters can only be detected by local probes such as neutron CEF

spectroscopy as outlined in the present work.

Financial support by the Swiss National Science Foundation is gratefully acknowledged.

-
- [1] J. D. Jorgensen, B. Dabrowski, P. Shiyou, D. G. Hinks, L. Soderholm, B. Morosin, J. E. Schirber, E. L. Venturini, and D. S. Girley, *Phys. Rev. B* **38**, 11 337 (1988).
 - [2] C. Chaillout, S. W. Cheong, Z. Fisk, M. S. Lehmann, M. Marezio, B. Morosin, and J. E. Schirber, *Physica (Amsterdam)* **158C**, 183 (1989).
 - [3] P. C. Hammel, A. P. Reyes, Z. Fisk, M. Takigawa, J. D. Thompson, K. H. Heffner, and S. W. Chong, *Phys. Rev. B* **42**, 6781 (1990).
 - [4] R. K. Kremer, E. Sigmund, V. Hizhnyakov, F. Hentsch, A. Simon, K. A. Müller, and M. Mehring, *Z. Phys. B* **86**, 319 (1992).
 - [5] P. G. Radaelli, C. U. Segre, D. G. Hinks, and J. D. Jorgensen, *Phys. Rev. B* **45**, 4923 (1992).
 - [6] V. Hizhnyakov, N. Kristoffel, and E. Sigmund, *Physica (Amsterdam)* **160C**, 119 (1989).
 - [7] V. J. Emery, S. A. Kivelson, and H. Q. Lin, *Phys. Rev. Lett.* **64**, 1989 (1990).
 - [8] Y. Kubo and H. Igarashi, *Phys. Rev. B* **39**, 725 (1989).
 - [9] A. Furrer, P. Allenspach, J. Mesot, U. Staub, H. Blank, H. Mutka, C. Vettier, E. Kaldis, J. Karpinski, S. Rusiecki, and A. Mirmelstein, *Eur. J. Solid State Inorg. Chem.* **28**, 627 (1991).
 - [10] A. Podlesnyak, V. Kozhevnikov, A. Mirmelstein, P. Allenspach, J. Mesot, U. Staub, A. Furrer, R. Osborn, S. M. Bennington, and A. D. Taylor, *Physica (Amsterdam)* **175C**, 587 (1991).
 - [11] J. Mesot, P. Allenspach, U. Staub, A. Furrer, H. Mutka, R. Osborn, and A. D. Taylor, *Phys. Rev. B* (to be published).
 - [12] P. Meuffels, B. Rupp, and E. Pörschke, *Physica (Amsterdam)* **156C**, 441 (1988).
 - [13] B. Rupp, E. Pörschke, P. Meuffels, P. Fischer, and P. Allenspach, *Phys. Rev. B* **40**, 4472 (1989).
 - [14] D. J. Werder, C. H. Chen, R. J. Cava, and B. Batlogg, *Phys. Rev. B* **37**, 2317 (1988).
 - [15] J. D. Jorgensen, Shiyou Pei, P. Lightfoot, Hao Shi, A. P. Paulikas, and B. W. Veal, *Physica (Amsterdam)* **167C**, 571 (1990).
 - [16] R. J. Cava, A. W. Hewat, E. A. Hewat, B. Batlogg, M. Marezio, K. M. Rabe, J. J. Krajewski, W. F. Peck, Jr., and L. W. Rupp, Jr., *Physica (Amsterdam)* **165C**, 419 (1990).
 - [17] S. Kirkpatrick, *Rev. Mod. Phys.* **45**, 574 (1973).
 - [18] M. S. Osofsky, J. L. Cohn, E. F. Skelton, M. M. Miller, R. J. Soulen, Jr., S. A. Wolf, and T. A. Vanderah, *Phys. Rev. B* **45**, 4917 (1992).
 - [19] P. Allenspach, A. Furrer, and B. Rupp, in *Progress in High Temperature Superconductivity*, edited by V. L. Aksenov, N. N. Bogolubov, and N. M. Plakida (World Scientific, Singapore, 1990), Vol. 21, p. 318.